

Peritumoral Hyperintense Signal on Post-contrast FLAIR Images Surrounding Vestibular Schwannomas Following Stereotactic Radiosurgery

Sandy T. Nguyen, John C. Benson, Girish Bathla, Paul J. Farnsworth, Matthew L. Carlson, Michael J. Link, John I. Lane

ABSTRACT

BACKGROUND AND PURPOSE: Prior investigations have noted the presence of peritumoral hyperintense signal (a “halo”) around vestibular schwannomas on postcontrast 3D T2 FLAIR images. This study evaluated this phenomenon in a cohort of patients undergoing stereotactic radiosurgery.

MATERIALS AND METHODS: A retrospective review was completed of consecutive patients with presumed vestibular schwannomas undergoing stereotactic radiosurgery. Tumor size, location, presence or absence of a peritumoral halo, and halo thickness were recorded. Images were reviewed for presence and size of peritumoral hyperintense signal on postcontrast 3D T2 FLAIR images before and after treatment.

RESULTS: Twenty-six patients were included in this study, 14 of which were female (54.0%). Average age was 62±12 years. Prior to treatment, a post-contrast 3D T2 FLAIR hyperintense peritumoral halo was seen in 85% of patients, averaging 0.8±0.4 mm in thickness. There was a higher incidence of peritumoral halo in post treatment patients (96%) than pre-treatment patients (85%) (p=0.017) with a mean follow up period of 1.2 years (SD, 0.35) from 11/12/2019 to 9/5/2023. The average halo thickness was also larger in post-treatment patients (average=1.4±0.4 mm) compared to pre-treatment patients (0.8±0.4 mm) (p<0.001). Average tumoral size did not significantly change following treatment (p=0.10).

CONCLUSIONS: Vestibular schwannomas treated with stereotactic radiosurgery are more likely to have a peritumoral halo on post-contrast 3D T2 FLAIR images, with larger halo size as compared to pre-treatment studies. Further study with a larger tumor cohort and longer follow-up will be necessary to determine if these findings are predictive of subsequent tumor shrinkage.

ABBREVIATIONS: VSs = vestibular schwannomas; SRS = stereotactic radiosurgery; CPA = cerebellopontine angle; IAC = internal auditory canal.

Received month day, year; accepted after revision month day, year.

From the Department of Radiology (S.T.N., J.C.B., G.B., P.J.F., J.I.L.), and Department of Otolaryngology-Head and Neck Surgery and Neurologic Surgery (M.L.C., M.J.L.), Mayo Clinic, Rochester, Minnesota, USA.

The authors declare no conflicts of interest related to the content of this article.

Please address correspondence to John C. Benson, MD, Department of Radiology, Mayo Clinic, 200 1st St SW, Rochester, Minnesota, 55905, USA; Benson.john3@mayo.edu.

SUMMARY SECTION

PREVIOUS LITERATURE: This is a novel investigation of peritumoral hyperintense signal (a “halo”) around vestibular schwannomas in a patient cohort undergoing stereotactic radiosurgery.

KEY FINDINGS: Treated vestibular schwannomas tend to have great incidence of peritumoral “halo” with increased thickness compared to pre-treatment lesions.

KNOWLEDGE ADVANCEMENT: Increased understanding of signal changes of vestibular schwannomas following SRS could relate to increased tumor permeability and may be a predictor of subsequent tumor shrinkage.

INTRODUCTION

Vestibular schwannomas (VSs) are benign nerve sheath tumors that account for 6-8% of all intracranial tumors and represent the most common tumor of the cerebellopontine angle (CPA). VSs classically arise within the internal auditory canal (IAC) and extend into the CPA with tumor growth.¹⁻² On imaging, treatment naïve VSs can either demonstrate homogenous or heterogeneous intra-tumoral enhancement and may contain hemorrhage or cystic changes. Edema of the adjacent parenchyma is seen in up to 40% of cases, particularly with large tumor size or rapid growth.³⁻⁴ Symptoms of VSs most commonly encompass ipsilateral hearing loss and tinnitus. With increasing size, tumors may exert mass effect on adjacent structures resulting in trigeminal symptoms, hydrocephalus, and ataxia.⁵

A recent study described the presence of peritumoral hyperintense signal or “halo” around VSs on postcontrast 3D T2 FLAIR images. The authors of that study opined that this halo represented local leakage of gadolinium into the peritumoral space, although the mechanism remains unknown.⁹ To date, however, investigation of this phenomenon has been limited, and restricted to treatment-naïve patients. As such, the current study sought to further our knowledge of this subject by comparing the incidence and thickness of peritumoral halos in patients undergoing stereotactic radiosurgery (SRS).

Eligibility Criteria

Local institutional review board (IRB) approval was received prior to study commencement. A retrospective review of patients with clinically presumed VSs was conducted based on imaging findings over a 4-year period (11/12/2019-8/23/2023). These tumors were treatment-naïve and subsequently underwent SRS. Treatment with SRS was planned with the 3D T1 post-contrast sequence co-registered to the contour of the 50% isodose line. Patients with dedicated IAC imaging prior to and following therapy were reviewed for appropriate pre- and post-contrast images for comparison. Patients were excluded for absence of necessary MR imaging sequences. Demographic information was acquired through the electronic medical record.

MR Imaging Protocol

Patients were scanned with either a 3T Siemens (Siemens AG, Munich, Germany) or GE (General Electric, Boston, MA, USA) scanner with multichannel phased array coils (and a 32 or 64-channel head coil). 23 of the 26 patients underwent evaluation with a Siemens scanner both prior to and following SRS. One patient prior to SRS and two patients following SRS were imaged via a GE scanner. Dedicated IAC imaging was performed utilizing axial 3D T1 sampling perfection with application optimized contrasts by using different flip angle evolution (SPACE sequence; Siemens) (TR = 600 ms, TE = 32 ms, data matrix = 192 x 192, acquisition time = 4 minutes), axial 3D T2 SPACE (TR = 1300 ms, TE = 184 ms, data matrix = 320 x 320, acquisition time = 3 minutes 55 seconds), axial 3D fat-saturated postcontrast T1 SPACE (TR = 600 ms, TE = 32 ms, data matrix = 192 x 192, acquisition time = 4 minutes), and axial postcontrast 3D T2 FLAIR (TR = 5000 ms, TE = 379 ms, data matrix = 192 x 192, inversion time = 1700 ms, acquisition time = 4 minutes 29 seconds). The FOV was 150 for these sequences.¹⁰ Images were acquired in the sequence noted above per institutional protocol and also include pre-contrast standard full brain sequences (i.e. axial fat-saturated pre-contrast T2 FLAIR and sagittal pre-contrast T1 FLAIR). Gadobutrol (Gadavist®) IV per weight-based table (0.1mmol/kg) administered via IV push for all the exams. Axial 3D fat-saturated postcontrast T1 SPACE and subsequently axial postcontrast 3D T2 FLAIR were acquired following contrast injection. The order of the sequences was kept the same for all performed studies.

Imaging Evaluation

Two experienced neuroradiologists (J.C.B., J.I.L.) performed the retrospective imaging review. The radiologists were blinded to the presence of recent treatment. VSs were evaluated for laterality – right or left – and location, described as in the internal auditory canal (IAC), cerebellopontine angle (CPA), or both. Prior to and following treatment, all VSs were measured in a single maximal axial dimension for size. If the VS involved both the IAC and CPA, the largest single axial dimension of the CPA component was measured for standardization. Presence or absence of a fundal cleft was also reported, as well as fundal cleft size between the lateral aspect of the VS and the IAC fundus.

VSs evaluated for presence or absence of a peritumoral hyperintense signal on postcontrast 3D T2 FLAIR images (“halo”), before and after SRS, through the overlaying and fusion features of our PACS system (Visage, version 7.1.18, Visage imaging, San Diego, CA). Axial postcontrast 3D T2 FLAIR images are fused and overlaid with both axial fat-saturated postcontrast T1W1 and axial T2 SPACE images (**Figure 1**). Pre-contrast T2 FLAIR and post contrast 3D T2 FLAIR were not directly comparable and therefore the halos could not be measured on pre-contrast images. Size or thickness of halo, if present, was measured through the differences in tumor size between the different sequences. The halos were measured perpendicular to the tumors. Although the halos were irregular in areas, the largest halo measurement for each tumor was recorded. Image subtraction also utilized to better detect differences between the tumor margins and the peritumoral halo. Whether the peritumoral hyperintense signal was confined to the fundus was recorded. Halo thickness was averaged between the two observer measurements. Any disagreements between the observers for categorical variables were resolved by consensus.

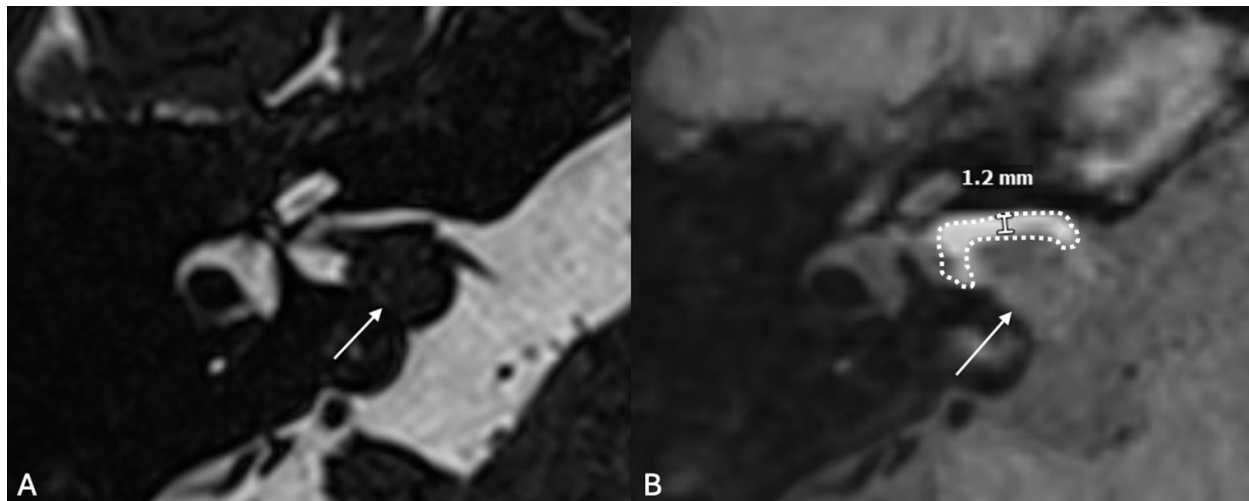


FIG 1. Evaluation and measurement of peri-tumoral halo. Axial T2 Space (A) and co-registered T2 Space and post-contrast 3D T2 FLAIR (B) images demonstrate a right-sided vestibular schwannoma (arrows) with peri-tumoral enhancement that is predominantly

along the anterior margin of the tumor (*dashed line*). Measurement of the halo was performed perpendicular to the tumoral margin.

Statistical Analysis

For all continuous variables, means and SDs were calculated. The Pearson's Chi-square test was used to calculate statistically significant associations between the continuous variables. The Student's t test was used to calculate statistical differences of the continuous variables. Cohen's kappa was used to calculate interrater reliability with categorical variables. P values less than 0.05 were statistically significant.

RESULTS

Twenty-six patients were included in the study, of which 14 were female (54.0%) and 12 were male (46.0%). Average age was 62 years old (SD 12). Fourteen tumors were right-sided (56.0%) and 12 were on the left (46%). Of these, 8 (31%) tumors were restricted to the IAC, 1 (4%) entirely situated in the cerebellopontine angle, and 17 (65%) involved both regions. The tumors were Koos 1-4: 7 Koos 1 (27%), 11 Koos 2 (42%), 5 Koos 3 (19%), and 3 Koos 4 (12%). Average follow up period was 1.2 (SD 0.35) years or on average 14 months for each patient following initial baseline imaging. Pre-treatment MRI studies performed immediately before treatment. Post procedural imaging acquired approximately 10 (SD 2.4) months following end of treatment. Pretreatment VSs measured 1.1±0.4 cm and posttreatment VSs measured 1.3±3.3 cm. Average tumoral size did not significantly change following treatment (p=0.10). Interobserver agreement on the presence of a halo prior to treatment was substantial (k = 0.63), whereas following treatment it was moderate (k = 0.56).

Peritumoral halo on postcontrast 3D T2 FLAIR images ("halo") was seen in 85% of patients prior to treatment, and 96% following SRS, with significant difference noted between pre- and post-treatment groups (p=0.017). Prior to treatment, peritumoral halos measured 0.8±0.4 mm in maximum thickness on average, which significantly increased in size following treatment (1.4±0.4 mm) (p<0.001). Four of the VSs did not demonstrate a peritumoral halo before SRS (15.0%). Of these 4, 3 developed halos following treatment.

A fundal cleft was observed in 21 (81%) patients, with an average cleft size of 1.7±1.1 mm. The cleft size did not significantly change following treatment (p=0.14). Peritumoral halo was restricted to the fundus in 18 (69.0%) patients prior to SRS. None of the post-treatment patients had a halo restricted to the fundus. There was no correlation between the change in halo thickness and Koos classification.

DISCUSSION

This study evaluated the changes in the incidence and thickness of peritumoral halos around VSs following SRS in a treatment-naïve cohort. The results indicate that peritumoral halos are more commonly seen around post-treatment tumors and are increased in thickness. The halos, when present, are also less likely to be restricted to the IAC fundus. Together, these findings indicate that the incidence, thickness, and locality of peritumoral halos around VSs change after SRS.

Stereotactic radiosurgery treatment combines delayed vascular and cytotoxic effects as described by Yang et. al. These delayed vascular effects pertain to radiation-induced damage to tumor nutrient vessels, critical for tumoral necrosis. The underlying abnormal vasculature of VSs is more susceptible to radiation-induced sequelae than normal vessels. Cytotoxic effects relate to DNA damage from gamma rays, generating oxygen free radicals and resultant strand breakage. The effects of SRS were studied on healthy rat brains, generating significant vascular permeability about the area of treatment and the formation of new, leaky blood vessels seen on Gd-DTPA dynamic contrast-enhanced MRI and T2*-weighted sequences.¹²

The most immediate implications of this study are that it offers further clues regarding the composition of peritumoral halos. Like the authors of the Benson et al. study, we hypothesize that the peritumoral halos could represent local extra-tumoral leakage of gadolinium. The observed changes in these halos following SRS might represent that there is a greater degree of gadolinium leakage after SRS. Although the findings might reflect increased tumoral permeability, it is important to mention that no additional references have theorized increased vascular permeability as the etiology of the halo sign and the appearance could also partly be due to accompanying inflammation. If that is the case, steroid use after treatment might have affected our results.

Steroids are not routinely prescribed in the early period after treatment. Although if a patient experiences a sudden sensorineural hearing loss in the post-SRS period (confirmed on audiogram), a course of steroids can be considered. In the uncommon case of a patient experiencing symptomatic brainstem edema after radiosurgery, steroids are used. In our cohort, no known steroid administration is documented to mitigate an inflammatory treatment response.

As first described, the peritumoral halos are often nonuniform in appearance and irregularly marginated. The authors of the original study on this concept hypothesized this irregularity could be explained by the trapping of gadolinium in the variably adhered and irregular arachnoid about the tumor.⁹ It is possible that SRS leads to increase permeability, and a larger concentration gradient of extravasated contrast, resulting in larger signal thickness. Extension of peritumoral halo beyond the IAC might also be related to the internal necrosis of tumor making it more "leaky". Post-SRS tumor necrosis is an important correlate of treatment effect and might have a correlation with the degree of increased peritumoral halo. Evaluation of this relationship was not within the scope of this study but is worthy of future analysis.

Next, as stated in the results, peritumoral halos were often restricted to the IAC in pre-treatment tumors but were observed circumferentially around the tumors in post-treatment patients. Most likely, this is because local gadolinium leakage is easier to observe in the IAC in the presence of a VS, where it is entrapped, or at least partially entrapped, by mass effect related to the VS. In post-treatment tumors, conversely, the increased permeability allows for observation of a halo even in regions that are not entrapped, such as the cerebellopontine angle and cerebellum (**Figures 2 and 3**).

It is interesting to speculate, that if indeed, the halo corresponds to gadolinium leakage, its increase following treatment could reflect increased tumor permeability and may be a predictor of subsequent tumor shrinkage, following SRS. Although we found no significant change in size of tumor after SRS in our small cohort, our follow up period was less than 2 years. A longer follow up period (potentially

at least 3 years as seen in a study performed by Lipski et. Al) may be needed to see treatment response as it relates to tumor control and shrinkage, despite increased halo thickness and possible associated tumor permeability presenting within 2 years following treatment. Further study with a larger number of tumors over a longer imaging interval will be needed to determine if this might prove to be the case.

This study has several limitations given its retrospective nature. The results are based on a small cohort and a larger sample size is needed to validate these findings as well as overall clinical significance. Longer follow up periods than what is seen in our cohort may also be helpful to evaluate for presence of absence of communicating hydrocephalus, change in tumor size, and temporal evolution of halo thickness and morphology as well as clinical impact relating to sensorineural hearing loss, tinnitus, and vertigo. Unlike in our prior investigations, patients were selected for availability of appropriate pre- and post-contrast imaging prior to and after treatment, which resulted in several patient exclusions for missing imaging. There are also inherent technical differences across multiple manufacturers, such as GE and Siemens, which can be more challenging in direct comparison. Finally, the small average halo thickness of reported measurements –between 0.4 and 1.5 mm before treatment and 0.4 and 2.6 mm after SRS – may be challenging due to pixel size on standard PACS measuring tools. It is worth noting that the voxel dimension is 0.78 mm (192 x 192 acquisition matrix with FOV 150) and the average increase in halo thickness from pre- to post- treatment was 0.6 mm and therefore smaller than the acquired voxel.

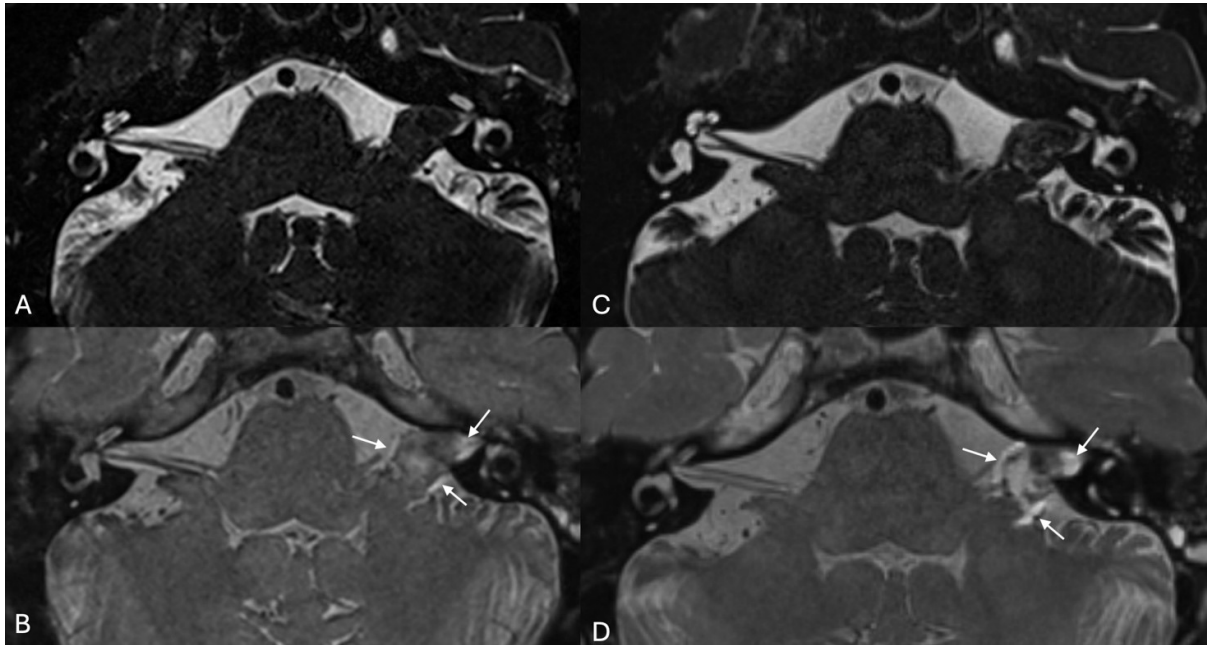


FIG 2. Increased size of a peritumoral halo in a 68-year-old female. Pre-radiosurgery axial T2 Space (A) and post-contrast 3D T2 FLAIR (B) images demonstrate a small halo located circumferentially around a left VS (arrows on B). Post-radiosurgery axial T2 Space (C) and post-contrast 3D T2FLAIR (arrows, D) images show that the halo has increased in size following treatment.

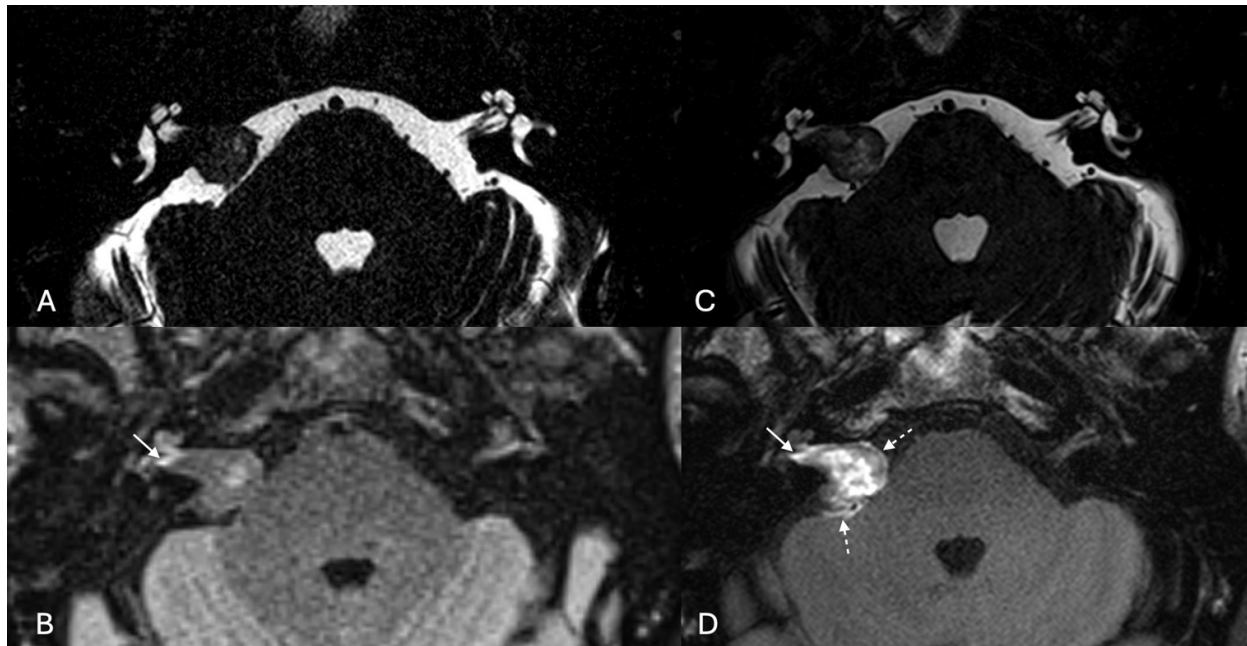


FIG 3. Increased halo size following SRS in a 66-year-old male. Pre-SRS axial T2 Space (A) and post-contrast 3D T2 FLAIR (B) images demonstrate minimal halo that is restricted to the IAC fundus (*solid arrow*, B). Following treatment, axial T2 Space (C) and post-contrast 3D T2 FLAIR (D) images show that the involvement of the fundus has increased (*solid arrow*, D). There is also new circumferential halo elsewhere (*dashed arrows*, D).

CONCLUSIONS

Vestibular schwannomas treated with stereotactic radiosurgery are more likely to have a peritumoral halo on post-contrast 3D T2 FLAIR images, with larger halo size as compared to pre-treatment studies. Further study with a larger tumor cohort and longer follow-up will be necessary to determine if these findings are predictive of subsequent tumor shrinkage.

REFERENCES

1. Lin EP, Crane BT. The management and imaging of vestibular schwannomas. *AJNR Am J Neuroradiol* 2017;38:2034–43
2. Connor SE. Imaging of the vestibular schwannoma: diagnosis, monitoring, and treatment planning. *Neuroimaging Clin N Am* 2021;31:451–71
3. Bonneville F, Savatovsky J, Chiras J. Imaging of cerebellopontine angle lesions: an update, Part 1: enhancing extra-axial lesions. *Eur Radiol* 2007;17:2472–78
4. Thamburaj K, Radhakrishnan VV, Thomas B, et al. Intratumoral microhemorrhages on T2*-weighted gradient-echo imaging helps differentiate vestibular schwannoma from meningioma. *AJNR Am J Neuroradiol* 2008;29:552–57
5. Gurewitz J, Schnurman Z, Nakamura A, et al. Hearing loss and volumetric growth rate in untreated vestibular schwannoma. *J Neurosurg* 2022;136:768–75
6. Tanaka Y, Kobayashi S, Hongo K, Tada T, Sato A, Takasuna H. Clinical and neuroimaging characteristics of hydrocephalus associated with vestibular schwannoma. *J Neurosurg*. 2003 Jun;98(6):1188-93. doi: 10.3171/jns.2003.98.6.1188. PMID: 12816262.
7. Fukuda M, Oishi M, Kawaguchi T, et al. Etiopathological factors related to hydrocephalus associated with vestibular schwannoma. *Neurosurgery* 2007;61:1186–92; discussion 1192–93
8. Al Hinai Q, Zeitouni A, Sirhan D, Sinclair D, Melancon D, Richardson J, Leblanc R. Communicating hydrocephalus and vestibular schwannomas: etiology, treatment, and long-term follow-up. *J Neurol Surg B Skull Base*. 2013 Apr;74(2):68-74. doi: 10.1055/s-0033-1333621. Epub 2013 Feb 7. PMID: 24436891; PMCID: PMC3699216.
9. Benson JC, Carlson ML, Lane JI. Peritumoral Signal on Postcontrast FLAIR Images: Description and Proposed Biomechanism in Vestibular Schwannomas. *AJNR Am J Neuroradiol*. 2023 Oct;44(10):1171-1175. doi: 10.3174/ajnr.A7979. Epub 2023 Aug 31. PMID: 37652582; PMCID: PMC10549947.
10. Benson JC, Carlson ML, Lane JI. MRI of the Internal Auditory Canal, Labyrinth, and Middle Ear: How We Do It. *Radiology*. 2020 Nov;297(2):252-265. doi: 10.1148/radiol.2020201767. Epub 2020 Sep 22. PMID: 32960730.
11. Yang SY, Kim DG, Chung HT, Park SH, Paek SH, Jung HW. Evaluation of tumour response after gamma knife radiosurgery for residual vestibular schwannomas based on MRI morphological features. *J Neurol Neurosurg Psychiatry*. 2008 Apr;79(4):431-6. doi: 10.1136/jnnp.2007.119602. Epub 2007 Aug 2. PMID: 17673492.
12. Constanzo J, Masson-Côté L, Tremblay L, Fouquet JP, Sarret P, Geha S, Whittingstall K, Paquette B, Lepage M. Understanding the continuum of radionecrosis and vascular disorders in the brain following gamma knife irradiation: An MRI study. *Magn Reson Med*. 2017 Oct;78(4):1420-1431. doi: 10.1002/mrm.26546. Epub 2016 Nov 10. PMID: 27851877.
13. Lipski SM, Hayashi M, Chernov M, Levivier M, Okada Y. Modern Gamma Knife radiosurgery of vestibular schwannomas: treatment concept, volumetric tumor response, and functional results. *Neurosurg Rev*. 2015 Apr;38(2):309-18; discussion 318. doi: 10.1007/s10143-014-0601-3. Epub 2014 Dec 19. PMID: 25519767.